Analysis of Dual LIDAR Placement for Off-Road Autonomy using MAVS

Christopher R. Hudson, Chris Goodin, Matthew Doude, and Daniel W. Carruth
Center for Advanced Vehicular Systems,
High Performance Computing Collaboratory (HPC^2),
Bagley College of Engineering,
Mississippi State University,
200 Research Blvd., Starkville, MS 39759.
Email: chudson@cavs.msstate.edu, cgoodin@cavs.msstate.edu,
mdoude@cavs.msstate.edu, dwc2@cavs.msstate.edu

***Abstract*—Two simulations were conducted using the Mississippi State University Autonomous Vehicle Simulator (MAVS) to evaluate the orientation of two M8 LIDAR units on an off-road autonomous vehicle project. The first simulation assesses the ability of the two LIDAR units to detect an object, in this case a Jersey barrier, at a significant distance away from the vehicle as it travels along a pre-defined path. The second simulation seeks to find an optimal orientation for the LIDAR units given their current position to maximize coverage of the terrain in the path of the vehicle. The results of the two simulations indicate that vertical placement of LIDAR units (0 degree rotation) provides less than ideal instantaneous coverage of obstacles and the ground. An 87 degree rotation provided the maximum single-pass coverage of the terrain along the travel path while also providing a good visualization of objects in the path of the vehicle, given the constraints of this project.**

I. Introduction

A large amount of research has focused on the integration of autonomous commercial and personal vehicles into the existing transportation infrastructure [1]. As these systems are being developed for real-world use, high-fidelity simulation environments are allowing for safe, inexpensive, and hardware-free prototyping and testing of control systems and sensor integration tasks [2][3]. Typical updates to existing software on autonomous and semi/autonomous adaptive driver assist technologies are thoroughly tested in simulation and are often subjected to millions of miles of simulated driving conditions prior to being deployed on vehicles. In 2017, Waymo, formerly Google's self-driving car project, reportedly completed 2.7 billion miles in simulation [2]. This ability to safely test the effects of changes on a system prior to deployment is critical to avoiding the potential effects of a system failure.

Simulation can provide a platform for predicting performance of sensor systems and advancing the capability of processing algorithms in on-road or off-road environments [4][5][6][7]. In 2017, Mississippi State University (MSU), kicked off a project to design and implement an off-road autonomous vehicle. The CAVS HALO project involves modifying a Subaru Forester and integrating on-board sensor packages to support autonomous behaviors in off-road conditions. The Forester is currently equipped with three M8 Quanergy

Fig. 1. LIDAR placement on HALO project vehicle.

LIDAR units for direct measurement of the operating environment [8]. Two of these LIDAR units are located at the front of the vehicle just below the headlights at 34.7 degrees off-axis from the centerline of the vehicle and one is mounted in the front center of the vehicles roof rack. This project seeks to leverage simulation to identify an optimal mounting angle for the two LIDAR units located at the front of the Forester. The goal of this analysis is to find a mounting angle that provides the best overall coverage of obstacles in the path of the vehicle and the ability to detect changes in the ground profile on the path of the vehicle as it moves through the off-road environment.

To complete this analysis, we leverage MSUs Center for Advanced Vehicular Systems (CAVS) new simulation environment, the Mississippi State University Autonomous Vehicle Simulator (MAVS). Two simulations investigating the two LIDAR units at the front of the vehicle were conducted using MAVS. The roof-mounted LIDAR was not considered in this analysis. The first simulation investigated the ability of the two LIDAR units to detect a standard precast concrete barrier at various distances with the LIDAR units mounted at different

angles. The second simulation investigated the ability of the two LIDAR units to profile the ground for different stop zones, determined according to stopping distances for a range of speeds.

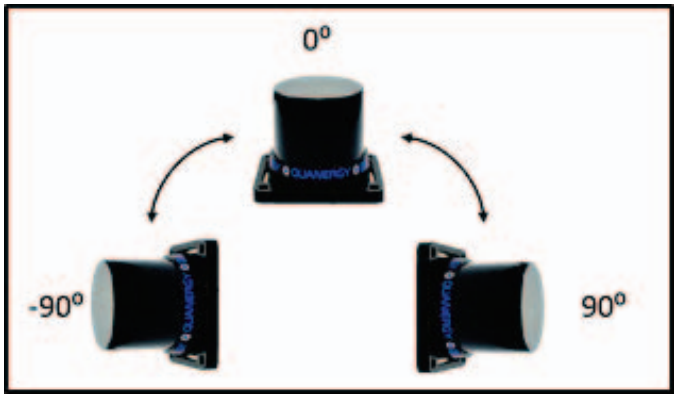

Fig. 2. LIDAR mount orientation.

II. Simulation Designs

Two simulations were conducted using MAVS in order to evaluate coverage of two LIDAR units according to target type (obstacles and ground) and orientation (mounting angle). All simulations were run on a computation server using 16 cores and 396 GB of memory. The position of the M8 LIDAR units relative to the vehicle frame was held constant for both simulations. Mounting angle was defined as the rotation of the LIDAR units around an axis parallel to the centerline of the vehicle (see Fig. 2). At -90 degrees, the top of the LIDAR units are oriented towards the body of the vehicle. At 90 degrees, the top of the LIDAR units are oriented away from the body of the vehicle. The LIDAR units were also rotated 34.7 degrees off-axis from the centerline of the vehicle. This angle was held constant across all simulations. Model parameters for the M8 Quanergy LIDAR units were defined based on specifications provided in manufacturer published data sheets [9]. No data on the beam divergence pattern was provided for the M8 Quanergy LIDAR units. As a substitution, a square divergence pattern consistent with the Velodyne HDL-64E was used.

Parameters	Specification
Min & Max horizontal angle	[-180, 180]
Horizontal resolution	0.06857
Min & Max vertical angle	[-18.22, 3.2]
Vertical resolution	3.06
Min range	1m
Max range	150m
Beam spot shape	Rectangular
Horizontal divergence	0.0033
Vertical divergence	0.0007
Mode	strongest

TABLE I
M8 Quanergy LIDAR Specifications

A. Simulation I

The first simulation assessed the ability of the two M8 LIDAR units to detect a standard precast concrete barrier in the path of the Forester at different distances. To simulate this, the simulated LIDAR units were placed 58 meters away from a New Jersey-shape precast concrete barrier, commonly referred to as a Jersey barrier [10]. Walls were placed 3 meters away from the centerline of the road. Once placed in the environment, a single scan of the environment was completed for each LIDAR unit starting at an angle of 90-degrees. Any LIDAR beams that collided with the concrete barrier were recorded. The angle of each LIDAR unit was then decremented by 1 degree and another scan was conducted. This process was repeated for all angles from 90-degrees to -90-degrees, at 1-degree increments. The rotation of the left and right LIDAR units were mirrored. After scans were completed for every test angle, the position of the Forester was advanced 2 meters and the process was repeated. This continued until the vehicle was 6 meters away from the concrete barrier.

B. Simulation II

The second simulation assessed the ability of the two M8 LIDAR units to profile the terrain located on the path of the vehicle. To accomplish this, the path in front of the vehicle was separated into four zones. These zones were based on a minimum required stopping distance at given speeds: 16.09 kph (10 mph) to 48.28 kph (30 mph). The first zone began at 1.45m (4.77 ft), the stopping distance for a vehicle under ideal conditions (dry and immediate no delay reaction) traveling at 16.09 kph (10 mph). This zone extended until the start of zone two which began at 3.27m (10.75 ft) (stopping distance for a vehicle traveling at 24.14 kph (15 mph)). The third zone began at 5.82m (19.11 ft), the stopping distance required for a vehicle traveling at 32.18 kph (20 mph). The third zone

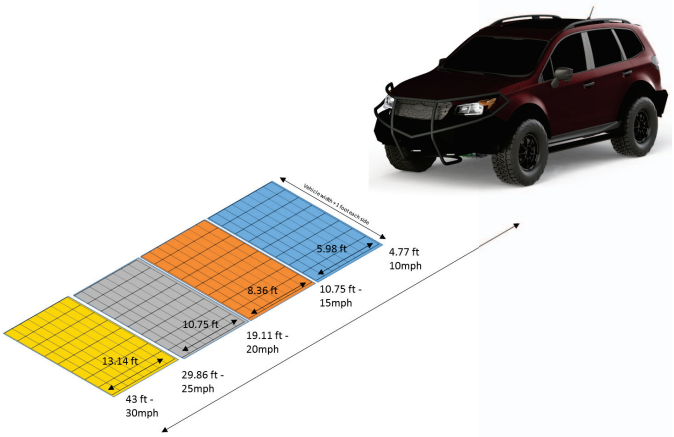

Fig. 3. Stop zone map.

extended to the start of zone four, which began at 9.10m (29.86 ft), the stopping distance for a vehicle traveling 40.23 kph (25 mph). This zone extended 13.10m (43 ft) from the vehicle, the

stopping distance required for a vehicle operating at 48.28 kph (30 mph). The overall width of the zones was held constant at the width of the vehicle + 0.3048m (1 ft) on either side.

III. Results

A. Simulation I

A total of 27 distances were checked, ranging from 6 meters to 58 meters in 2-meter increments. As the vehicle approached the concrete barrier, the number of points which fell on the barrier increased. At 10m away from the concrete barrier, the two LIDAR units at an angle of 0 degrees returned a combined 1249 points. At 90 degrees, the two LIDAR units returned a combined 1227 points. At -90 degrees, the two LIDAR units returned a combined 644 points.

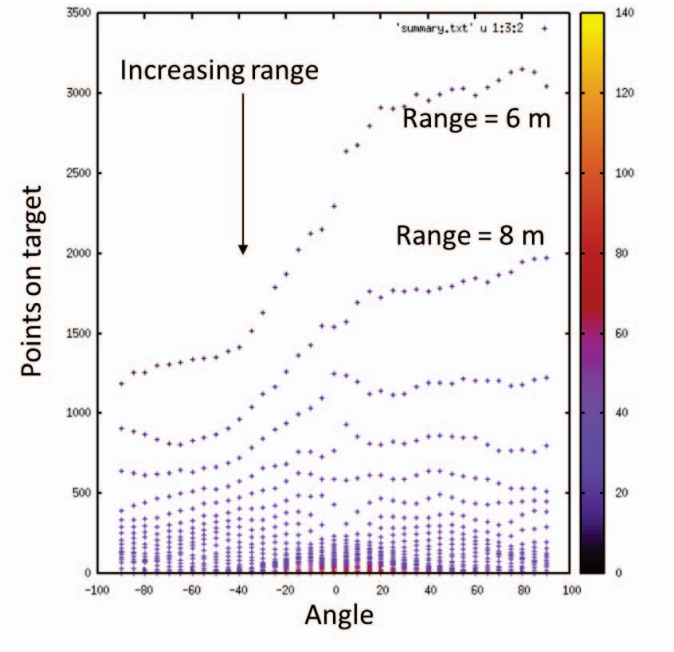

Fig. 4. Points on target by angle.

B. Simulation II

The coverage of the four path zones was calculated for every angle between -90 and 90 in one degree increments. First, we consider coverage by zone (see Table II). In zone 1, the highest percent coverage was provided by units mounted at an angle of -26 degrees with 17.08% of zone 1 covered. In zone 2, the highest percent coverage was provided was by units mounted at an angle of 84 degrees with 13.82% of zone 2 covered.

Angle	Percent Coverage	Angle
Zone 1	17.08	-26
Zone 2	13.82	84
Zone 3	7.4	-31 or 49
Zone 4	3.4	-21

TABLE II
TOTAL PATH COVERAGE BY ZONE

In zone 3, the highest percent coverage was provided was by units mounted at an angle of -31 or 49 degrees, both of which covered 7.4% of zone 3. Finally, in zone 4, units mounted at an angle of -21 degrees provided the most coverage (3.4% of zone 4).

When looking at total area coverage (summing percent coverage across all four zones; see Table III), mounting the units at an angle of 87 degrees provides the best overall coverage of all four zones with a total of 40.12% of the area covered.

Angle	Sum Coverage
82	39.92
83	40.04
84	40
86	40
87	**40.12**
88	40
89	39.98

TABLE III
TOTAL PATH COVERAGE BY ANGLE

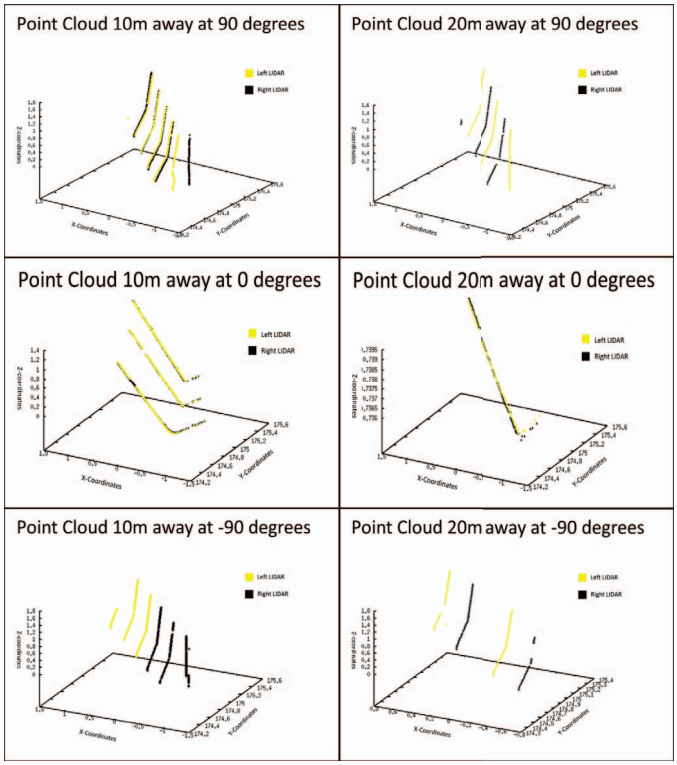

Fig. 5. Visualization of returns for concrete barrier at -90, 0, and 90 degrees.

IV. Discussion

These results provide insight into the influence of angular placement on coverage provided by LIDAR units on vehicles. The simulation results indicate that placing a LIDAR at -90 degrees (mounted inward towards the vehicle) provides the lowest level of information possible about an approaching

target. While the data suggests that placing the LIDAR units at an angle of 0 degrees provides the highest number of returns for the concrete barrier obstacle, the units mounted at 90 degrees provided similar results. These results become even more interesting when a 3D scatter plot of the data (see Fig. 5) is generated. The scatter plots depict LIDAR point clouds generated by a scan by both LIDAR units at angles of 90 degrees and 0 degrees.

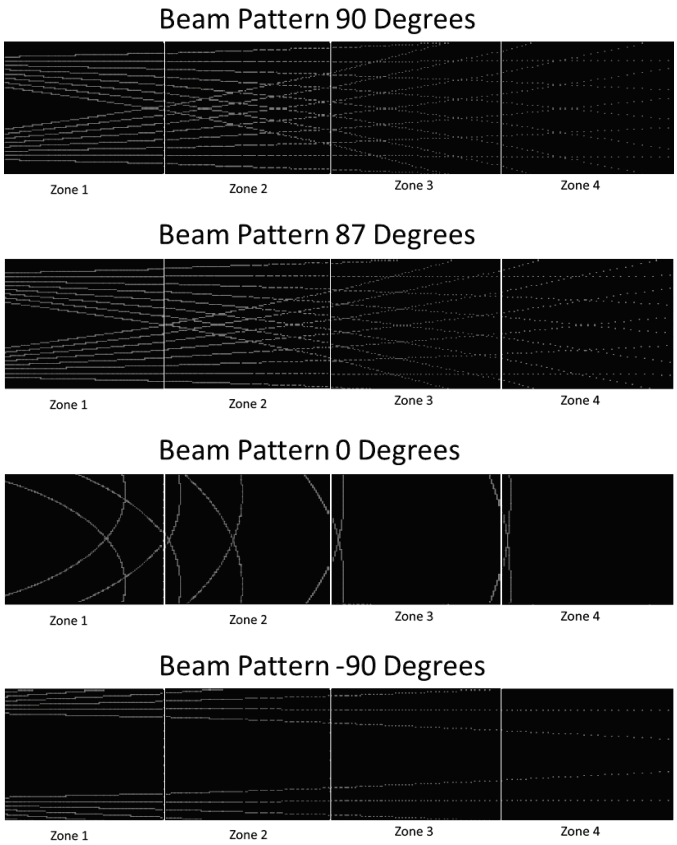

Fig. 6. Visualization of beam contact with ground by angle.

When these plots are generated, it becomes clear that, while the LIDAR units mounted at 0 degrees provide more data points, those data points are far more clustered than the data points returned by the LIDAR units mounted at 90 degrees. Additionally, the scatter plots reveal features of the concrete barrier not seen by the LIDAR angled at 0 degrees. Most notably, the increased thickness at the base of the Jersey barrier is visible in the 90 degree scans. Since the LIDAR readings are being sampled from different parts of the object due to the angle of the LIDAR at 90 degrees, the data generated by these scans is arguably more useful than the data provided by the 0 degree LIDAR units.

The second simulation, which looked exclusively at the ground coverage provided by the two LIDAR units when mounted at different angles, provided more insight into the optimal orientation for the two units. As the percent coverage was calculated, it became clear that the optimal placement of the sensors depends on prioritization of the zones. Given that the distance between scans greatly increases as you move away from the vehicle, it was no surprise to see lower percent coverage in zones further away from the vehicle. What was interesting, however, was the combined total percent coverage across all four zones. When looking at coverage for all four zones, it was surprising to see that the optimal coverage occurred between 82 and 88 degrees (not a typical orientation for LIDAR units). In fact, it appears that the optimal angle to maximize the coverage of the ground ahead of the vehicle is at 87 degrees, covering 40.12% across all four zones. Visualization of the beams spread across the four zones (see Fig. 6) reveals the difference in beam pattern created by rotating the LIDAR a few degrees.

These results indicate that the optimal orientation for mounting the two forward facing M8 LIDAR located at the front of the Subaru Forester for the HALO project, based on the current analysis, is an angle of 87 degrees. This angle will provide the best overall ground coverage for the path directly in front of the vehicle as well at provide an effective view of obstacles such as the concrete barrier in the path of the vehicle. This analysis does not examine the visibility of obstacles or paths to the right and left of the vehicle. However, the top-mounted third LIDAR is expected to provide good forward-looking coverage for these areas.

V. Future Work

Moving forward there are several avenues of investigation that can be explored using similar simulations. They are enumerated below:

- Investigate the effects of angular placement on reducing the shadowing effect of objects in the path of the vehicle.
- Determine the maximum size object which could hide between scans based on position and orientation of the LIDAR sensors.
- Incorporate a non-uniform ground for the path, ideally based on real terrain.
- Expand the definition of the ground zones to account for space to the left and right of the vehicle.
- Collect real world data from the HALO project to compare to simulated results.
- Update simulation to investigate possible LIDAR placements as well as possible mounting angles to achieve the best possible view of both incoming obstacles and the terrain.

References

[1] D. J. Fagnant and K. Kockelman, *Preparing a nation for autonomous vehicles: opportunities, barriers and policy recommendations,* Transportation Research Part A: Policy and Practice, vol. 77, pp. 167181, 2015.

[2] Waymo.com, *"Waymo On the road"*, 2018. Available: https://waymo.com/ontheroad.

[3] J.L. Pereira and R.J. Rossetti, *"An integrated architecture for autonomous vehicles simulation."*, In Proceedings of the 27th annual ACM symposium on applied computing, pp. 286-292, 2012.

[4] D.R. Chambers, J. Gassaway, C. Goodin, P.J. Durst, *"Simulation of a multispectral, multicamera, off-road autonomous vehicle perception system with virtual autonomous navigation environment (vane),"* Electro-Optical and Infrared Systems: Technology and Applications XII;and Quantum Information Science and Technology. International Society for Optics and Photonics, pp. 964802, Vol. 9648, 2015.

[5] J.T. Carrillo, C.T. Goodin, A.E. Baylot, *"Nir sensitivity analysis with the vane."* Infrared Imaging Systems: Design, Analysis, Modeling, and Testing XXVII. International Society for Optics and Photonics, pp. 98200I, Vol. 359, 2016.

[6] J.E. Davis, A.E. Bednar, C.T. Goodin, P.J. Durst, D.T. Anderson, C.L. Bethel, *"Computational intelligence-based optimization of maximally stable extremal region segmentation for object detection,"* Signal Processing, Sensor/Information Fusion, and Target Recognition XXVI. International Society for Optics and Photonics, pp. 102000V, Vol. 10200, 2017.

[7] C. Goodin, R. Kala, A. Carrrillo, L.Y. Liu, *"Sensor modeling for the virtual autonomous navigation environment,"* Sensors, pp. 1588-1592, 2009.

[8] B. Schwarz, *"LIDAR: Mapping the world in 3D,"* Nature Photonics, pp. 429, 4, 2010.

[9] *M8 LIDAR SENSOR*, Quanergy Systems, 2015

[10] ASTM C825-06(2011), *"Standard Specification for Precast Concrete Barriers"*, ASTM International, West Conshohocken, PA, 2011.